Supplementary Material

Modification of Magnetic Graphene Oxide by An Earth-Friendly Deep Eutectic Solvent to Preconcentrate Ultratrac Amounts of Pb(II) and Cd(II) in Legume Samples

Melika Hejazikhah and Parastoo Jamshidi *

School of Chemistry, College of Science, University of Tehran, Tehran P.O. Box 14155-6455, Iran
* Correspondence: parastoo.jamshidi@ut.ac.ir

Characterization

Table S1. summarizes the data.

Table S1. FT-IR analysis.

mGO		**EgLiCl-mGO**	
Bond	Peak	Bond	Peak
Stretching O-H	3380 cm^{-1}	Stretching O-H	3430 cm^{-1}
Carbonyl C=O	1730 cm^{-1}	Bending O-H	1640 cm^{-1}
Aromatic C=C	1630 cm^{-1}	CH_2 stretching	2914 cm^{-1}
Bending O-H	1360 cm^{-1}	CH_2 scissor	1460 cm^{-1}
Aromatic C-C	1220 cm^{-1}	CH_2 wagging	1350 cm^{-1}
Alkoxy C-O-C	1050 cm^{-1}	CH_2 twisting	1258 cm^{-1}
Stretching CH_2	2880 cm^{-1}	Li-O	1300 cm^{-1}
Carbonyl C=O	1730 cm^{-1}	Fe-O	700 cm^{-1}
Fe–O	700 cm^{-1}		

Adsorption isotherm

Figure S1 shows that by increasing the concentrations of Pb(II) and Cd(II), the adsorption capacity of EgLiCl-mGO increased.

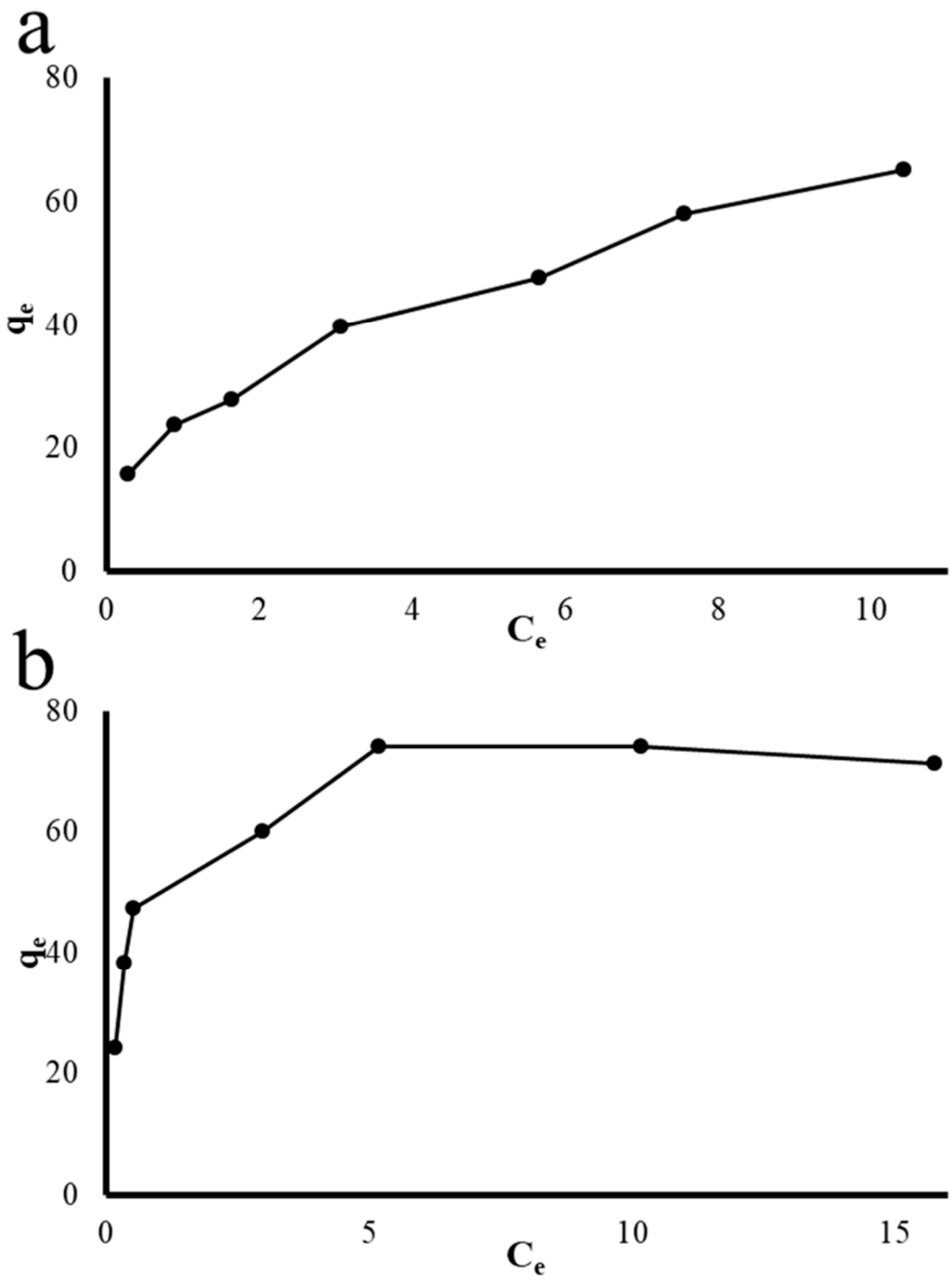

Figure S1. Effect of initial concentrations of **a** Pb(II) and **b** Cd(II) on the adsorption capacity of EgLiCl-mGO

Figure S2 shows the Langmuir model of Pb(II) and (b) Cd(II) adsorptions onto EgLiCl-mGO.

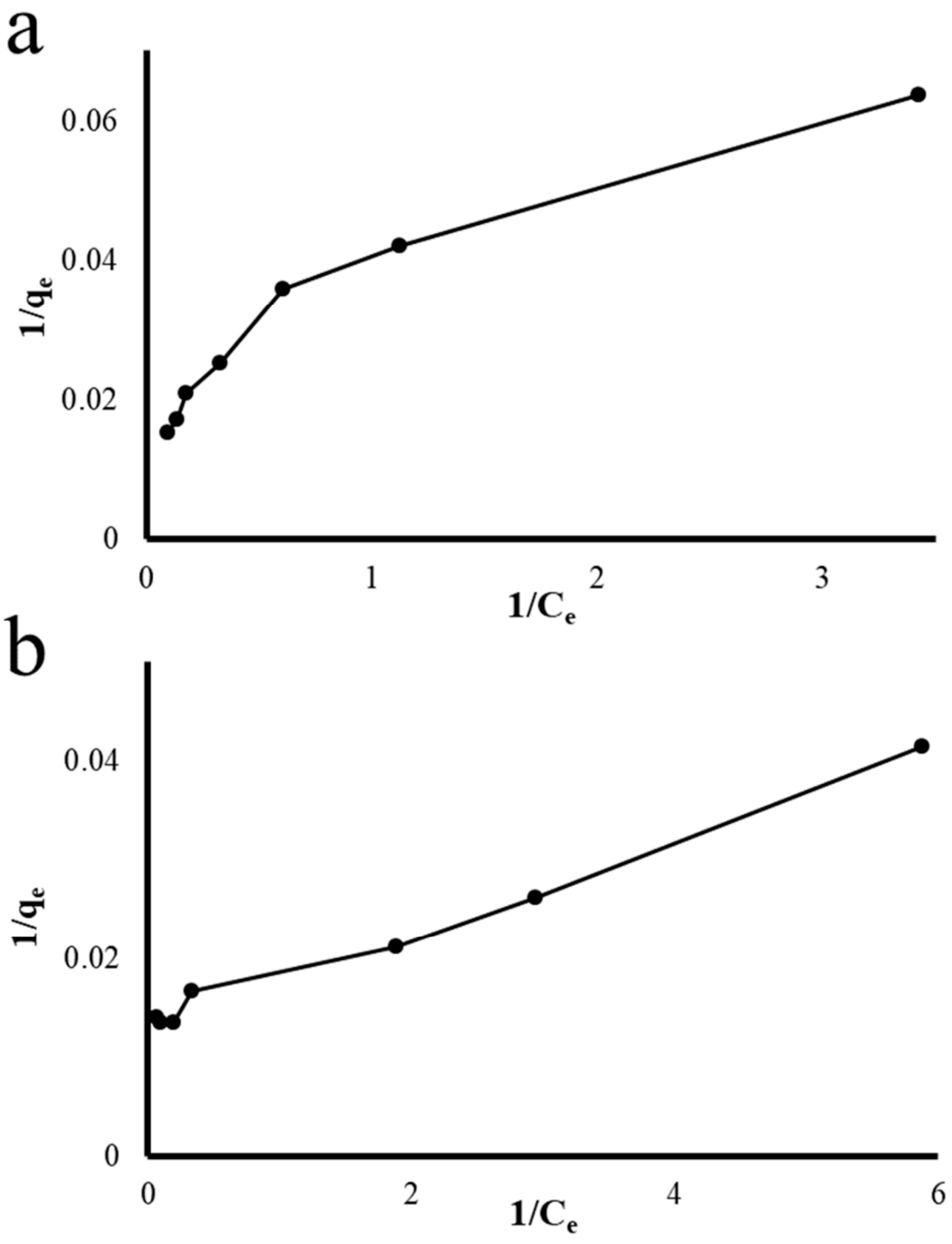

Figure S2. The Langmuir model of **a** Pb(II) and **b** Cd(II) adsorptions onto EgLiCl-mGO.

Figure S3 shows the Freundlich model of Pb(II) and (b) Cd(II) adsorptions onto EgLiCl-mGO.

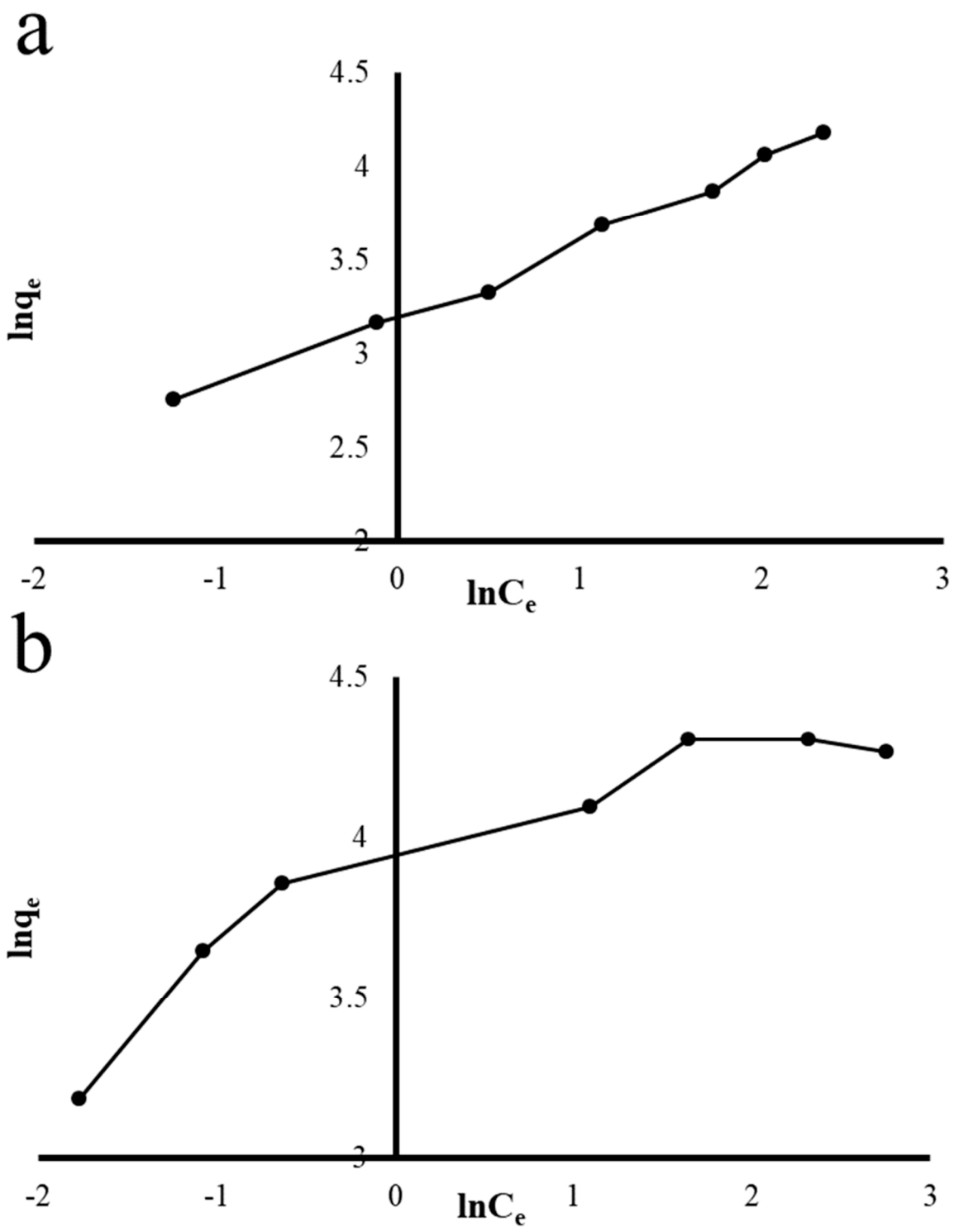

Figure S3. The Freundlich model of **a** Pb(II) and **b** Cd(II) adsorptions onto EgLiCl-mGO.

Figure S4 shows the Temkin model of Pb(II) and (b) Cd(II) adsorptions onto EgLiCl-mGO.

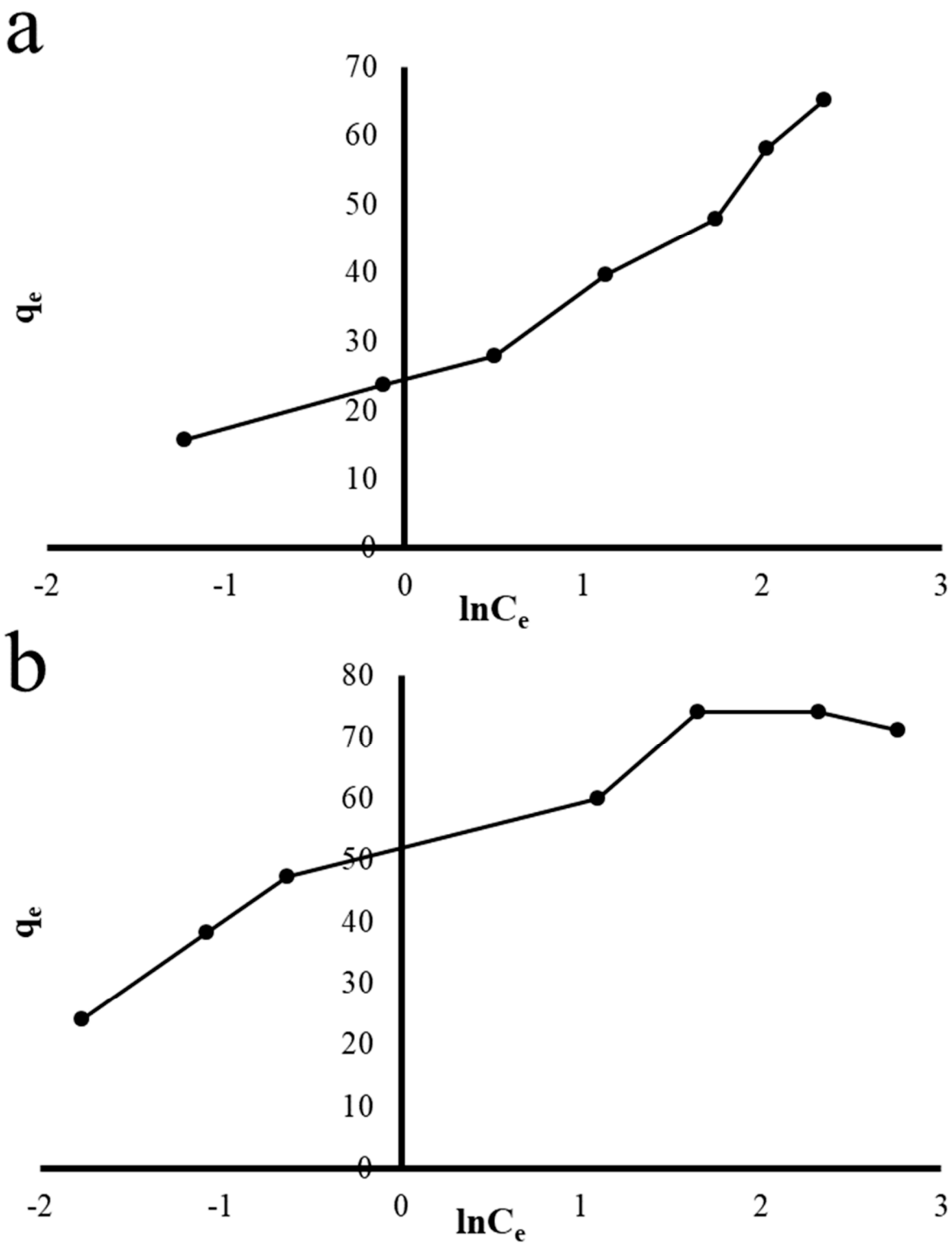

Figure S4. The Temkin model of **a** Pb(II) and **b** Cd(II) adsorptions onto EgLiCl-mGO.

Figure S5 shows the Halsey model of Pb(II) and (b) Cd(II) adsorptions onto EgLiCl-mGO.

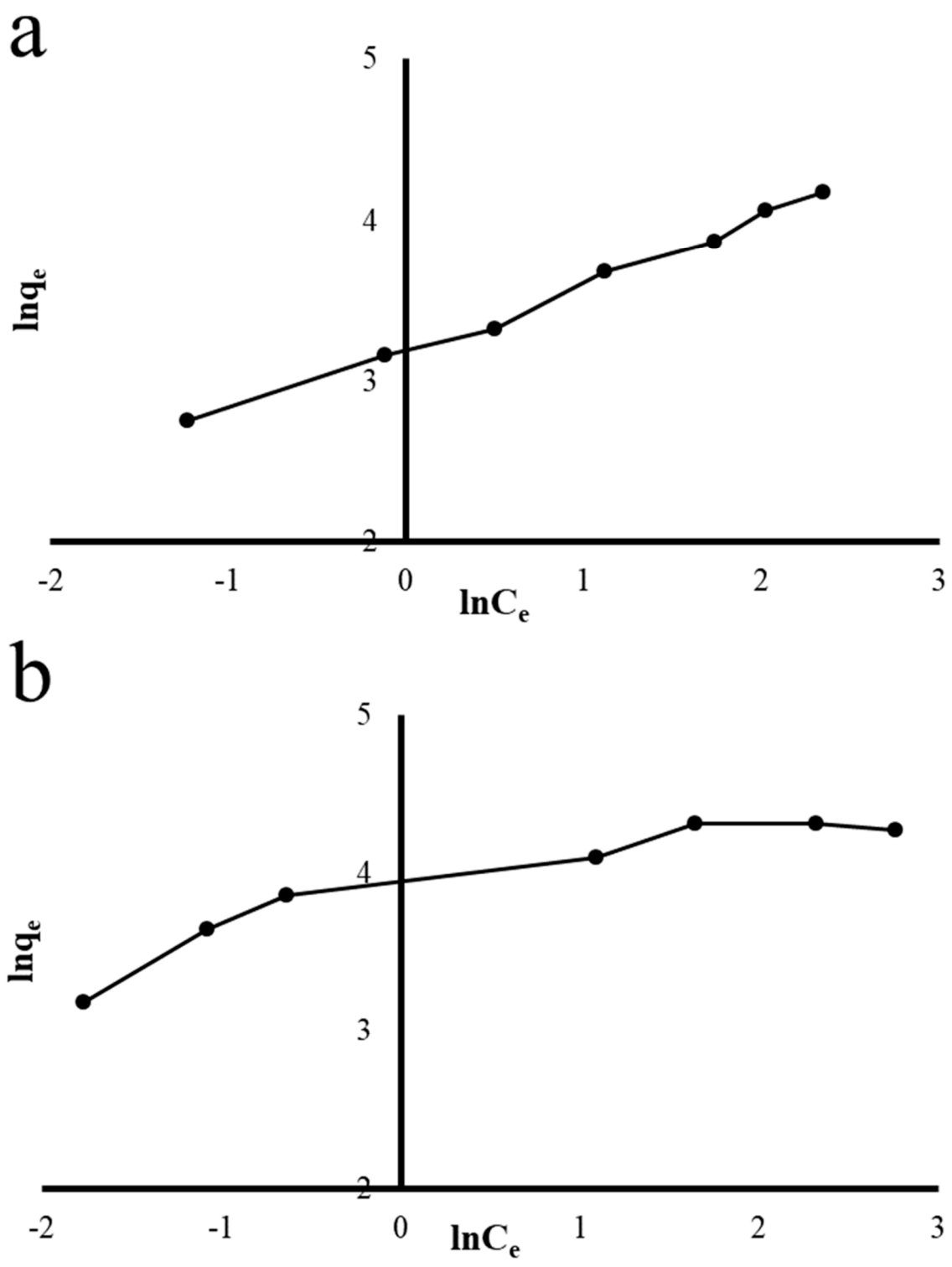

Figure S5. The Halsey model of **a** Pb(II) and **b** Cd(II) adsorptions onto EgLiCl-mGO.

Figure S6 shows the Elovich model of Pb(II) and (b) Cd(II) adsorptions onto EgLiCl-mGO.

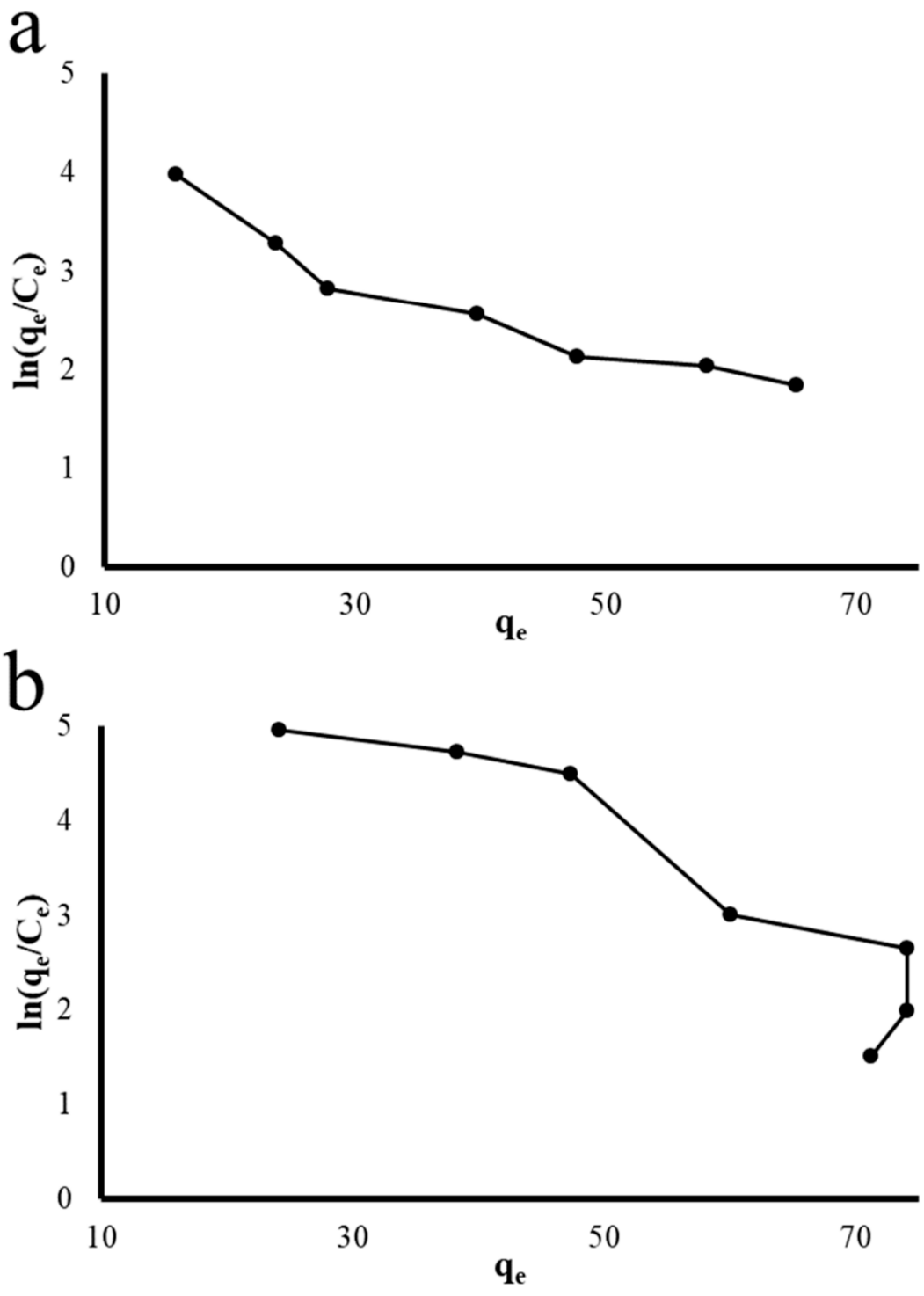

Figure S6. The Elovich model of **a** Pb(II) and **b** Cd(II) adsorptions onto EgLiCl-mGO.

Adsorption kinetic

Figure S7 shows the first-order kinetic model of Pb(II) and (b) Cd(II) adsorptions onto EgLiCl-mGO.

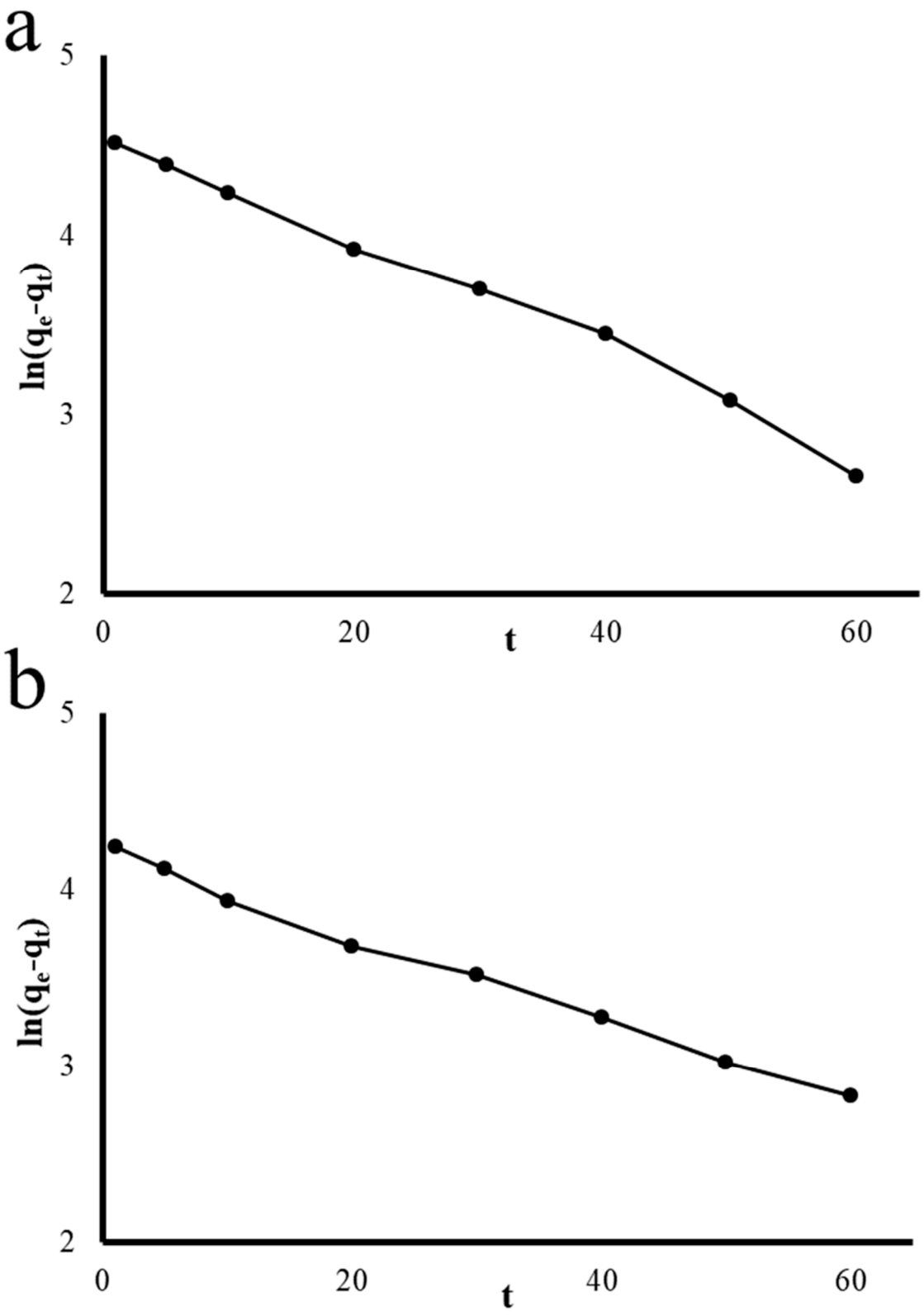

Figure S7. The first-order kinetic model of **a** Pb(II) and **b** Cd(II) adsorptions onto EgLiCl-mGO.

Figure S8 shows the second-order kinetic model of Pb(II) and (b) Cd(II) adsorptions onto EgLiCl-mGO.

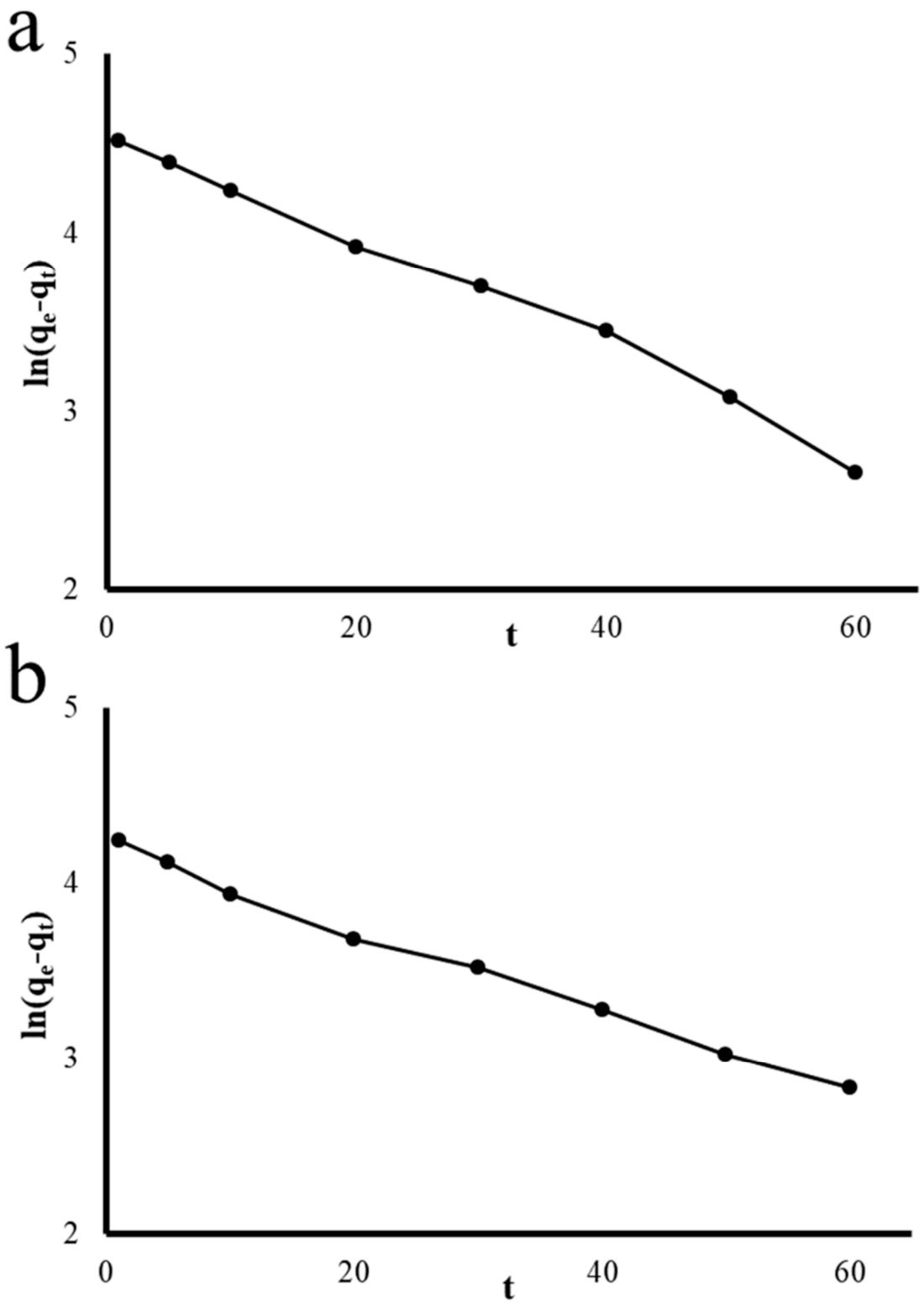

Figure S8. The first-order kinetic model of **a** Pb(II) and **b** Cd(II) adsorptions onto EgLiCl-mGO.

Adsorption thermodynamic

Thermodynamic parameters, enthalpy and entropy for the adsorption of Pb(II) and Cd(I) onto EgLiCl-mGO were calculated according to Figure S9.

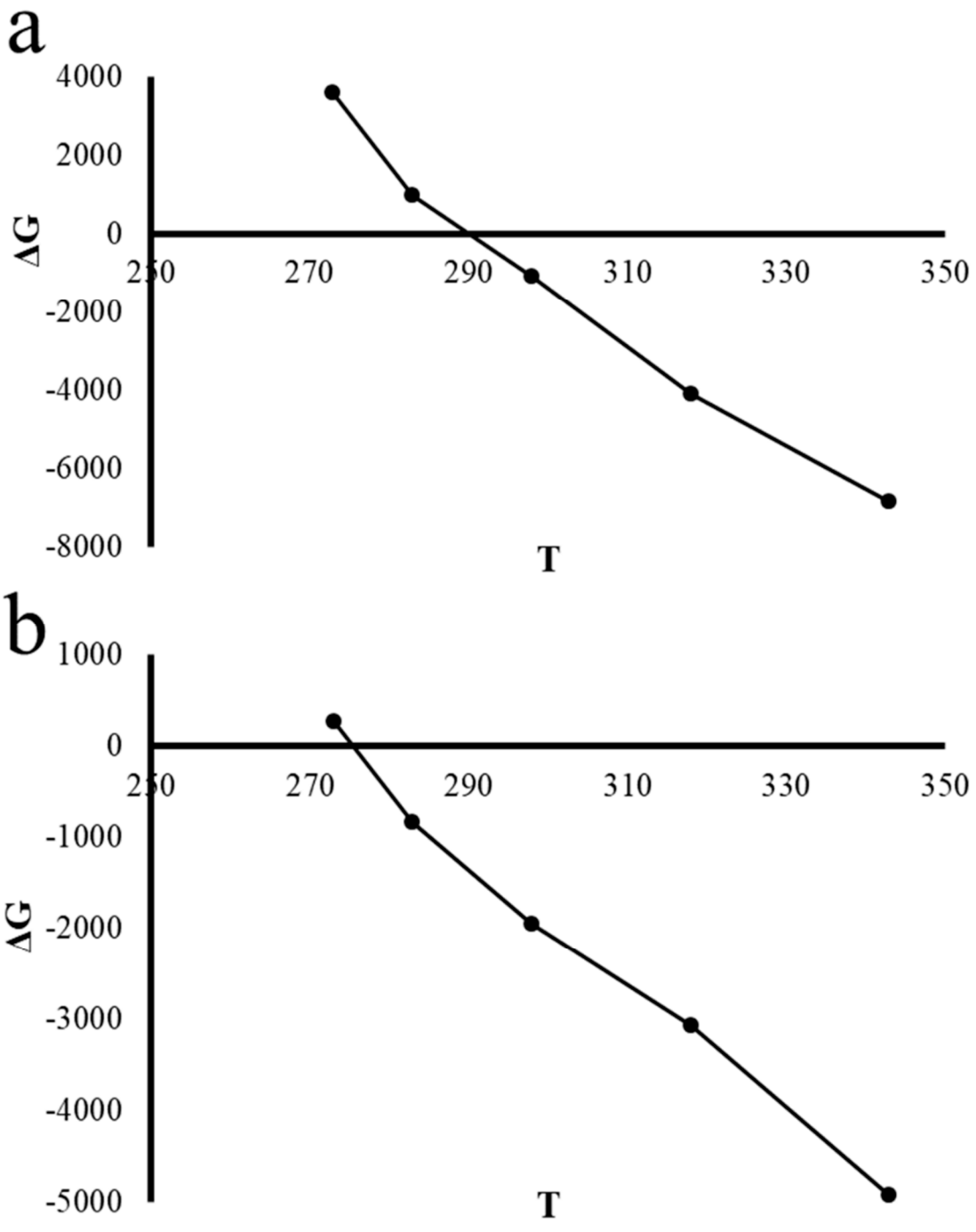

Figure S9. Thermodynamic parameters, enthalpy and entropy for the adsorption of **a** Pb(II) and **b** Cd(II) onto EgLiCl-mGO.